Polyhedron 78 (2014) 46–53

Contents lists available at ScienceDirect

Polyhedron

journal homepage: www.elsevier.com/locate/poly

Modified glassy carbon electrode with AuNPs using *cis*-[RuCl(dppb)(bipy)(4-vpy)]$^+$ as crossed linking agent

Vanessa F. Ferreira [a,1], Cássio R.A. Do Prado [a], Carolina M. Rodrigues [a], Larissa Otubo [b], Alzir A. Batista [c], José W. da Cruz Jr. [c], Javier Ellena [d], Luís R. Dinelli [a], André L. Bogado [a,*]

[a] Faculdade de Ciências Integradas do Pontal, Universidade Federal de Uberlândia, Rua vinte, 1600, CEP 38304-402 Ituiutaba, MG, Brazil
[b] Centro de Ciência e Tecnologia de Materiais, Instituto de Pesquisas Energéticas e Nucleares, Av. Prof. Lineu Prestes 2242, Cidade Universitária, CEP 05508-000 São Paulo, SP, Brazil
[c] Departamento de Química, Universidade Federal de São Carlos, CP 676, CEP 13565-905 São Carlos, SP, Brazil
[d] Instituto de Física de São Carlos, Universidade de São Paulo, CP 780, 13560-970 São Carlos, SP, Brazil

ARTICLE INFO

Article history:
Received 21 February 2014
Accepted 15 April 2014
Available online 23 April 2014

Keywords:
Gold nanoparticles
Ruthenium complexes
Electrostatic interaction
Modified glassy carbon electrode
Acetaminophen detection

ABSTRACT

This work links aspects of non-covalent interaction among gold nanoparticles (AuNPs) and ruthenium complexes, which were used to modify the surface of the glassy carbon electrode (GCE), without the necessity of a sulfur substrate with a covalent bond between gold–sulfur (Au–S), to keep the AuNPs onto the surface of the electrode. The AuNPs were synthesized by the method of encapsulation by citrate conferring on them a negative charge. The ruthenium complex [RuCl(dppb)(bipy)(4-vpy]$^+$ was synthesized by ligand exchange in its coordination sphere, giving it a positive charge. A thin film of [RuCl(dppb)(bipy)(4-vpy)]$^+$ was generated onto the surface of glassy carbon electrode (GCE), using cyclic voltammetry, under potential cycling between −0.9 and −2.4 V, to produce the CGE–Ru$^+$ electrode. Afterward, the GCE–Ru$^+$ electrode was kept in a colloidal suspension of AuNPs for 1 h to incorporate them onto the surface of GCE–Ru$^+$ by electrostatic interaction. The resulting electrode GCE–Ru–AuNPs was finally washed with water to remove the excess of AuNPs and it was used to acetaminophen detection by cyclic voltammetry. To find the optimum analysis conditions of the modified electrode, studies were conducted to understand; which were: the number of cyclic voltammograms to produce the film, dip-coating time in AuNPs, pH, scan rate and repeatability. The Ru–AuNPs aggregates were analyzed by UV–Vis spectroscopy (UV–Vis), Fourier transform infrared spectroscopy–attenuated total reflectance (FTIR–ATR), nuclear magnetic resonance of phosphorus ($^{31}P\{^1H\}$ NMR), cyclic voltammetry (CV); scanning electron microscopy with energy dispersive spectroscopy (SEM–EDS) and transmission electron microscopy with energy dispersive spectroscopy (TEM–EDS). The X-ray structure of [RuCl(dppb)(5,5′-Me-bipy)(4-vpy)](PF_6) was determinate.

1. Introduction

More than 70000 publications have appeared on gold nanoparticles (AuNPs) to date, which have been producing recent developments in the synthesis and functionalization of AuNPs [1,2]. AuNPs can be prepared by both "top down" and "bottom up" approaches, where the control of size and shape of particles, as well as further functionalization is more effortlessly obtained in bottom up method, by chemical or biological reduction of individual molecules. This chemical reduction method involves two steps: nucleation and successive growth. When the nucleation and successive growth are completed in the same process, it is called *in situ* synthesis; otherwise it is called *seed-growth* method [1].

In this context, the "*in situ*" Turkevich–Frens [3,4] method, to obtain ca. 10 to 150 nm AuNPs, and the Brust–Schiffrin [5,6] method, to obtain hydrophobic AuNPs with diameters in 1 to ca. 8 nm ranges are still major synthetic routes [2].

Stabilization and functionalization of AuNPs has been extensively reviewed in AuNPs obtained from both, *in situ* or *seed-growth* method. Three kids of widely used methods to functionalization of AuNPs are: electrostatic interaction, specific recognition and covalent coupling [2].

AuNPs and functionalized AuNPs have been used for a wide range of application in many fields of knowledge. Only for illustration they are applied at: chemiluminescence sensors [7]; catalysis

* Corresponding author. Address: Rua vinte, 1600, Bairro Tupã, CEP 38.304-402 Ituiutaba, MG, Brazil. Tel.: +55 (34) 3271 5251; fax: +55 3271 5246.
E-mail address: albogado@pontal.ufu.br (A.L. Bogado).
[1] Present address: Instituto de Química de São Carlos, Universidade de São Paulo, CP 780, 13560-970 São Carlos, SP, Brazil.

http://dx.doi.org/10.1016/j.poly.2014.04.024
0277-5387/

in liquid phase [8–9]; hybrid nanobiomaterials [9–11]; biodiagnostics [12] and plasmonic sensors [13].

Most of the techniques reported for immobilizing ligands to AuNPs surfaces are based on Au–S covalent bond formation between the ligands and the gold atoms on the particle surfaces. This approach necessitates the use of sulfur containing ligand, i.e., thiol, disulfide and thiolester [9–11]. Nanoparticles functionalized with groups that provide affinity sites for the binding of biomolecules have also been used for the specific attachment of proteins and oligonucleotides [2]. Electrostatic interaction, non-covalent interaction or physical adsorption immobilization of specimen for AuNPs probes are simple processes with the benefits of time saving and reduced complexity of ligand preparation. Its relative simplicity gives this approach certain advantages over the complex covalent immobilization or specific recognition methods.

Non-covalent interactions are considerably weaker than covalent interactions, which can range between ca. 150 to 450 kJ mol^{-1} for single bonds. The term "non-covalent" includes a wide range of attractions and repulsions, which consist of ion–ion (200–300 kJ mol^{-1}), ion-dipole (50–200 kJ mol^{-1}), dipole–dipole (5–50 kJmol^{-1}), hydrogen bonding (4–120 kJ mol^{-1}), cation-π (5–80 kJ mol^{-1}), π–π (0–50 kJ mol^{-1}), van der Waals (<5 kJ mol^{-1}) and hydrophobic interaction related to solvent–solvent interaction energy [14].

The strongest non-covalent interaction, ion–ion and ion–dipole interaction have been used to produce modified electrodes by electrostatic interaction of anionic surface of AuNPs and cationic species. Wang and coworkers [15,16] describes a method for effective immobilizations of cationic ruthenium complexes on an electrode surface. Willner and co-workers [17,18] reported the construction, via electrostatic cross-linking, an electroactive multilayer electrode by simultaneously depositing anionic AuNPs and oligocationic cyclophanes. In both cases a donor S compound was used to cross-link the AuNPs with a derived indium tin oxide (ITO) electrode surface.

Recently our group described an electroactive carbon paste modified electrode, constructed by electrostatic interaction of AuNPs and a cationic complex of ruthenium, without S donor compounds [19]. Importantly, the produced nanocomposites did not include thiol-containing compounds, which could potentially decrease the catalytic activity of ruthenium in electrochemical reactions. Herein is described a new strategic route to incorporate AuNPs onto the surface of a glassy carbon electrode (GCE), using the [RuCl(dppb)(bipy)(4-vpy)]$^+$ as cross link agent between GCE and AuNPs.

2. Experimental

2.1. Reagents

All reactions were carried out under an argon atmosphere using standard Schlenk techniques. $RuCl_3{\cdot}xH_2O$, $H[AuCl_4]$, triphenylphosphine (PPh_3), 1,4-bis(diphenylphosphino)butane (dppb), 2, 2′-bipyridine (bipy), 5,5′-dimethyl-2,2′-bipyridine (5,5′-Me-bipy), pyridine (py), 4-vinylpyridine (4-vpy), and sodium citrate were purchased from Aldrich and used as received. Reagent grade solvents were distilled prior to use. The [RuCl(dppb)(bipy)(py)](PF_6) (**1**) and [RuCl(dppb)(bipy)(4-vpy)](PF_6) (**2**) were prepared as described previously [20–24]. Herein we will be discussing only unpublished results about these complexes. The *cis* designation used here is related to the position of the bidentate ligands.

2.2. Instrumentation

The NMR spectra of the compounds were performed at Universidade Federal de São Carlos, São Carlos (SP). They were acquired with a Bruker DRX-400 spectrometer (9.4 T) equipped with a 5 mm inverse probe head. Samples for $^{31}P\{^1H\}$ experiments were prepared under on inert atmosphere and measured at room temperature, with methylene chloride (CH_2Cl_2) as solvent and a D_2O capillary. Chemical shifts were reported with respect to the phosphorus signal in 85% phosphoric acid (H_3PO_4).

The microanalyses were performed at Universidade Federal de São Carlos, São Carlos (SP), using a FISONS CHNS-O, mod. EA 1108 Element analyzer.

Optical spectra were recorded on a Perkin Elmer model lambda 25 spectrophotometer with 1 cm quartz cell between 300 and 800 nm and FTIR spectra were recorded in an ATR apparatus with diamond cell support or conventional KBr cell of 0.2 mm length with a Jasco FTIR 4000 spectrometer in the 4000–400 cm^{-1} range.

Electrochemical data were obtained using a potentiostat/galvanostat μ-autolab type III. Solutions of the complexes (10^{-3} mol L^{-1}) were prepared in dichloromethane (CH_2Cl_2) using 10^{-3} mol L^{-1} tetrabutylammonium hexafluorophosphate (TBAH) as the supporting electrolyte. Measurements were made with a three-electrode configuration cell. A platinum foil was used as the working and auxiliary electrodes and Ag/AgCl, 0.10 mol L^{-1} TBAH in CH_2Cl_2 as the reference electrode. Under the conditions used, E^0 for the one-electron oxidation of [Fe(η^5-C_5H_5)$_2$], added to the test solutions as an internal calibrant, is +0.43 V.

Field emission scanning electron microscopy (FE-SEM) images and energy-dispersive spectroscopy (EDS) analysis were obtained using a JEOL JSM 6701F coupled with an EDS detector. The sample powder was directly dispersed on a SEM sample-holder using a conductive carbon paint. Transmission electron microscopy (TEM) images were obtained using a JEOL JEM 2100 (200 kV) equipped with a scanning TEM unit (STEM) and an EDS detector. The TEM sample were dispersed in isopropanol and dropped on a 400 mesh copper grid coated with a collodion film.

2.3. X-ray diffraction data

Crystals of [RuCl(dppb)(5,5′-Me-2,2′-bipy)(4-vpy)]PF_6 (**3**) were grown by slow evaporation of a dichloromethane/diethyl ether solution. The crystals were mounted on an Enraf-Nonius Kappa-CCD diffractometer with graphite-monochromated Mo Ka (l = 0.71073 Å) radiation. The final unit-cell parameters were based on all reflections. Data were collected with the COLLECT program; [25] integration and scaling of the reflections were performed with the HKL DENZO-SCALEPACK software package [26]. Absorption correction was carried out by the Gaussian method [27]. The structure was determined by direct methods with SHELXS-97 [28]. The model was refined by full-matrix least squares on F^2 by means of SHELXL-97 [29]. All hydrogen atoms were stereochemically positioned and refined with a riding model. The ORTEP view shown in Fig. 2 was prepared with ORTEP-3 for Windows [30]. Hydrogen atoms on the aromatic rings were refined isotropically, each one with a thermal parameter 20% greater than the equivalent isotropic displacement parameter of the atom to which it was bonded. The data collection and experimental details are summarized in Table 1, and the selected bond distances and angles are given in the caption of Fig. 2.

2.4. Synthesis of [RuCl(dppb)(5,5′-Me-bipy)(4-vpy)](PF_6) (3)

The *cis*-[$RuCl_2$(dppb)(5,5′-Me-bipy)] was prepared according to literature methods [31,32]. Excess of 5,5′-Me-bipy (0.160 g; 0.87 mmol) was added to a dark-green solution (0.500 g; 0.58 mmol) of [$RuCl_2$(dppb)PPh_3] [33], in 100 mL of CH_2Cl_2. The solution was refluxed for 48 h under Ar and the resulting red solution was then reduced to 1–2 mL, and Et_2O was added to precipitate the product, which was collected by vacuum filtration, washed with hexane (3 × 5 mL), Et_2O (6 × 5 mL), and dried under

Table 1
summarizes crystal data and provides data collection and refinement parameters.

Empirical formula	$[RuC_{47}H_{47}ClN_3P_2]$ PF_6
Formula weight	997.31
T (K)	293(2)
Wavelength (Å)	0.71073
Crystal system	orthorhombic
Space group	*Pbca*
Unit cell dimensions	
a (Å)	14.669(3)
b (Å)	20.499(3)
c (Å)	29.401(6)
V (Å^3)	8841(3)
Z	8
D_{calc} (Mg/m^3)	1.499
Absorption coefficient (mm^{-1})	0.587
$F(000)$	4080
Crystal size (mm)	0.16 × 0.07 × 0.05
Reflections collected	46980
Independent reflections (R_{int})	8675 (0.0969)
Completeness to θ = 26.02°	99.7%
Absorption correction	Gaussian
Final R indices [$I > 2\sigma(I)$]	R_1 = 0.0473, wR_2 = 0.0986
R indices (all data)	R_1 = 0.1074, wR_2 = 0.1177

vacuum. Yield: 0.44 g (86%). *Anal.* Calc. for $C_{40}H_{40}ClN_2P_2Ru$: C, 61.38; H, 5.15; N, 3.58. Found. C, 61.24; H, 5.22; N, 3.68%. $^{31}P\{^1H\}$ NMR (162 MHz, CH_2Cl_2/D_2O) δ(ppm) 45.4 (d) and 31.8 (d) (d = doublets, $^2J_{p-p}$ = 32.7 Hz).

The *cis*-[$RuCl_2$(dppb)(5,5′-Me-bipy)] (0.050 g; 0.057 mmol) was dissolved in 20 mL of CH_2Cl_2 and 0.043 mL (0.400 mmol) of 4-vinylpyridine was added to the red solution. Also, 0.022 g (0.114 mmol) of KPF_6 dissolved in 1.0 mL of methanol was added to the same solution. The mixture was stirred for 24 h, at room temperature, and then reduced to 1–2 mL, and Et_2O was added to precipitate the product, which was collected by vacuum filtration, washed with H_2O (4 × 5 mL), and Et_2O (5 × 5 mL), and dried under vacuum. Yield: 0.51 g (92.5%). *Anal.* Calc. for $C_{46}H_{47}ClN_3P_3F_6Ru$: C, 56.07; H, 4.81; N, 4.26. Found. C, 55.31; H, 4.80; N, 4.54%. $^{31}P\{^1H\}$ NMR (162 MHz, CH_2Cl_2/D_2O) δ(ppm) 37.13 (d) and 36.16 (d) (d = doublets, $^2J_{p-p}$ 34.83 Hz). The complex presents a quasi-reversible cyclic voltammogram in CH_2Cl_2, 10^{-3} mol L^{-1} Ru, 0.1 mol L^{-1} TBAP, scan rate 100 mV s^{-1}, at room temperature, with E_{ox} = 1200 mV and $E_{1/2}$ = 1125 mV, close to those found for similar chlorine complexes containing dppb, diimines and N-heterocyclic as ligands [20,21,32,34–38].

2.5. Preparation of gold nanoparticles (AuNPs)

AuNPs with a diameter of 10–18 nm were prepared by citrate reduction of H[$AuCl_4$] in aqueous solution according to a well-known method described by Frens [3]. In brief, 20 μL of solution containing H[$AuCl]_4$ (Au 58%) was added in 100 mL of water. The resulting solution was brought to reflux, and 3 mL of sodium citrate solution (1%) was introduced while stirring. The solution was then kept boiling for another 30 min, while the colors change from yellow to deep blue to red. Finally, the solution was left to cool to room temperature.

2.6. Aggregates of gold nanoparticles with ruthenium complexes

A typical experiment using [RuCl(dppb)(bipy)(py)](PF_6) is described: (71.1 mg; 75.1 μmol) of cationic ruthenium complex was dissolved in acetone (10 mL) under magnetic stirring at room temperature. After complete dissolution, it was transferred to a stock solution of AuNPs in water (100 mL, 0.5 mmol L^{-1}), which was previously synthesized. Therefore, the formation of a quantitative brown precipitate occurred. It was collect by centrifugation, washed three times with water, and then dried under vacuum.

2.7. Preparation of modifier electrode

The [RuCl(dppb)(bipy)(4-vpy)]$^+$ was linked on the surface of the glassy carbon electrode (GCE) by adsorption and reduction of 4-vinylpirydine group, which produced the glassy carbon–Ru^+ electrode (GCE–Ru^+). It was used a conventional cell containing a single compartment, a working GCE (2 mm Ø), a Pt counter electrode, and an Ag/AgCl electrode as reference. Ten voltammograms were carried out between −2.4 and 2.0 V with scan rate of 100 mV s^{-1} of a solution of [RuCl(dppb)(bipy)(4-vpy)](PF_6) (6,0 mg; 6.2 μmol) and TBAH (0.1 mol L^{-1}) in dichloromethane (10 mL). The GCE–Ru^+ electrode was introduced in a colloidal suspension of citrate-stabilized gold nanoparticles, with average diameter of about 14 nm ($AuNPs^-$, 0.05 mmol L^{-1} containing 9.9 mg of Au) within 60 min at room temperature. The characteristic interaction of GCE–Ru^+ and $AuNPs^-$ has produced a bimetallic modified electrode (GC–Ru–AuNPs), which was used to acetaminophen detection.

The GCE–Ru^+ can be also prepared with *in situ* generation of [RuCl(dppb)(bipy)(4-vpy)]$^+$ from *cis*-[$RuCl_2$(dppb)(bipy)] in the presence of excess of 4-vinypiridine (5 eq. related to ruthenium precursor), using the same configuration in the electrochemical cell. The chlorine ligand exchange by 4-vinypiridine has formed the same cationic complex containing ruthenium, which was linked on the surface of GCE.

3. Results and discussion

3.1. Syntheses and non-covalent interaction between AuNPs and ruthenium complexes (Ru–AuNPs)

The [RuCl(dppb)(bipy)(4-vpy)](PF_6) was prepared by ligand exchange from *cis*-[$RuCl_2$(dppb)(bipy) as ascribed by Batista and co-workers [20]. Experimental and theoretical study of the kinetics of dissociation in the *cis*-[$RuCl_2$(dppb)(bipy)] revealed that only the chloride *trans* to the phosphorus atom of the dppb ligand was dissociated, even in the presence of excess of monodentate ligand, such as monopyridine and functionalized monopyridine (Fig. 1).

Presence of more bulky group bonded in the N–N donor group, such as 5,5′-dimethyl-2,2′-bipyridine (5,5′-Me-bipy) produces the *cis*-[$RuCl_2$(dppb)(5,5′-Me-bipy)], and it also lost the chloride coordinated *trans* to P atom of dppb to produce a cationic complex containing ruthenium in the presence of 4-vpy. Suitable crystals of [RuCl(dppb)(5,5′-Me-bipy)(4-vpy)](PF_6) were obtained by slow evaporation of a dichoromethane/diethyl ether solution. The data collection and experimental details are summarized in Table 1 (Section 2), and selected bond distances and angles are given in the caption of Fig. 2.

The X-ray structural analysis of the complex [RuCl(dppb)(5,5′-Me-bipy)(4-vpy)](PF_6) shows that the chloride is *trans* to one of the 2,2′-bipyridine nitrogens (N2) and the 4-vinylpyridine is *trans* to one of the phosphorus atoms (P1). The Ru–N(1) (2.213 (3) Å) distance is longer than the Ru–N(2) bond (2.067 (3) Å), as expected, since the 4-vinylpyridine is a monodentate ligand, while the 2,2′-bipyridine is bidentate. In this case, the bidentate ligand is more tightly bonded to the metal center. On the other hand, the distance Ru–P(2) (2.3436 (10) Å), Ru–P(2) *trans* to N(3), is longer than the distance Ru–P(1) (2.3186 (11) Å), Ru–P(1) *trans* to N(1), since the 2,2′-bipyridine affects the P–Ru bonds *trans* to it more effectively than does the monodentate 4-vinylpyridine ligand. The bond distances and angles listed in the caption of the Fig. 2 are in the range expected for ruthenium biphosphine complexes [22,24,35–42]. Similar behavior was observed for the complexes containing

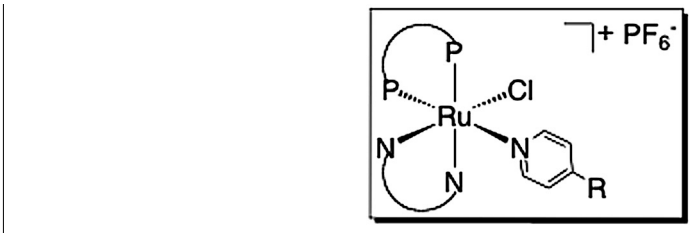

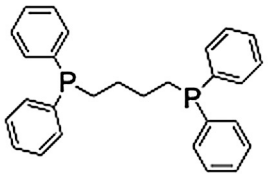

P-P = 1,4-bis(diphenylphosphyno)butane (dppb)

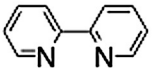

N-N = 2,2'-bipyridine (bipy)

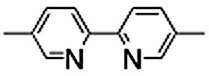

N-N = 5,5'-dimethyl-2,2'-bipyridine (5,5'-Me-bipy)

Complex	P-P	N-N	R
1	dppb	bipy	H
2	dppb	bipy	$-\underset{H}{C}=CH_2$
3	dppb	5,5'-Me-bipy	$-\underset{H}{C}=CH_2$

Fig. 1. General structures of complexes studied in this work as PF_6 salts.

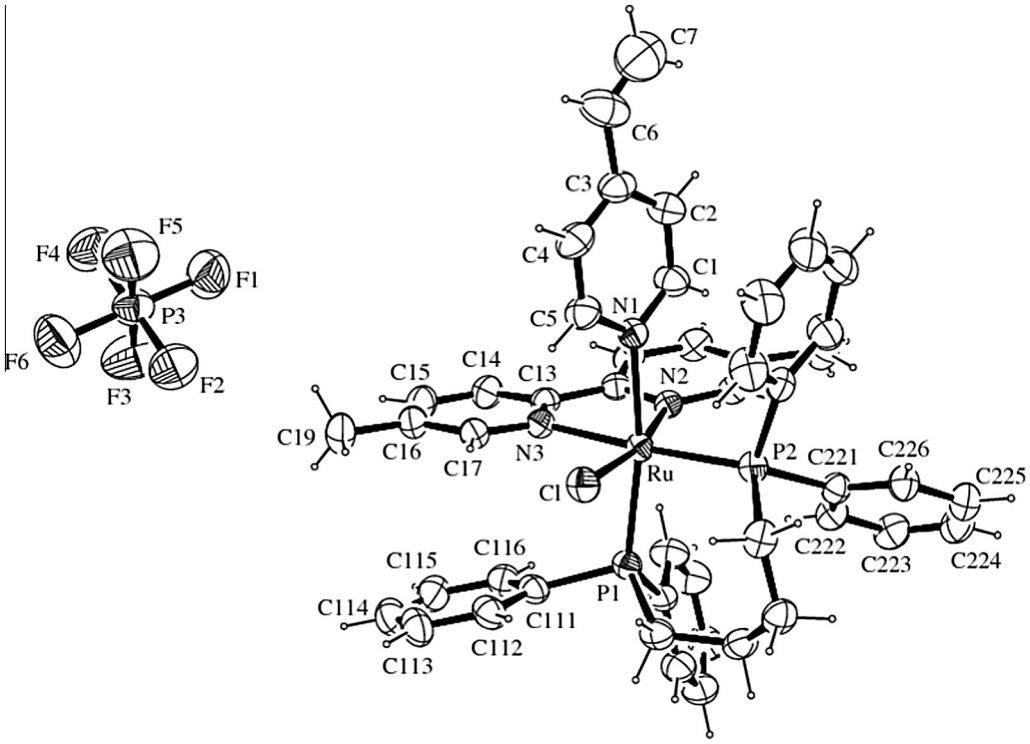

Fig. 2. ORTEP view and atomic numbering of [RuCl(dppb)(5,5′-Me-bipy)(4-vpy)](PF_6) showing the atoms labeling and 50% probability ellipsoids. Bond lengths (Å): Ru–N2 2.067 (3), Ru–N3 2.119 (3), Ru–N1 2.213 (3), Ru–P1 2.3186 (11), Ru–P2 2.3436 (10), Ru–Cl 2.4315 (9). Bond angles (°): N2–Ru–N3 77.54 (11), N2–Ru–N1 84.87 (11), N3–Ru–N1 83.13 (11), N2–Ru–P1 99.88 (8), N3–Ru–P1 89.91 (8), N1–Ru–P1 170.57 (8), N2–Ru–P2 101.80 (8), N3–Ru–P2 176.78 (8), N1–Ru–P2 93.67 (8), P1–Ru–P2 93.31 (4), N2–Ru–Cl 168.81 (8), N3–Ru–Cl 92.69 (8), N1–Ru–Cl 88.59 (8), P1–Ru–Cl 85.38 (3), P2–Ru–cl 87.65 (3).

4-methylpyridine and 4-phenylpyridine, as previously reported [33,39,43,44]. In all three complexes, the dissociated chloride was always the one *trans* to a phosphorus atom in the precursor *cis*-[$RuCl_2$(P-P)(bipy)] or *cis*-[$RuCl_2$(P-P)(5,5′-Me-bipy)] {where P-P = aromatic biphosphine}, as expected, given the stronger *trans* effect of the phosphorus atom and in accordance with the X-ray structures.

In order to apply these kinds of complexes as cross-link agents between glassy carbon electrode and AuNPs, the [RuCl(dppb)(bipy)(4-vpy)](PF_6) was prepared as previously described in the literature [20]. Cyclic voltammetry of [RuCl(dppb)(bipy)(4-vpy)](PF_6) has shown an oxidation potential (E_{ox}) at 1.19 V and a reduction potential (E_{red}) at 1.06 V due the redox pair Ru^{III}/Ru^{II}, with half wave potential ($E_{½}$) at 1.10 V. It also suggests a exchange between chlorine (π-donor group) and 4-vpy (π-acceptor group) in the *cis*-[$RuCl_2$(dppb)(bipy)], producing a cationic ruthenium complex, with increasing of potentials. The *cis*-[$RuCl_2$(dppb)(bipy)] has voltammetric parameters much more cathodic than the [RuCl(dppb)(bipy)(4-vpy)](PF_6) {E_{ox} = 0.64 V, E_{red} = 0.567 and $E_{½}$ = 0.54 V} [45].

Infrared data of [RuCl(dppb)(bipy)(4-vpy)](PF_6) revealed the characteristics bands of their ligands, dppb, bipy and 4-vpy. These aromatic ligands show a stretch at the 1435–1904 cm^{-1} range, which represents the C=C bonds, and the counter ion (PF_6) show a strong band at 853 cm^{-1}, due the P–F stretching.

Recently, we and others have been demonstrating the non-covalent interaction between AuNPs and cationic specimen [16–19] with different application in many fields of knowledge. The process of interaction between cationic ruthenium complexes Ru^+ and the negative surface of gold nanoparticles ($AuNPs^-$) can be accompanied by optical measurements [19].

Fig. 3 shows the plasmon band absorption of AuNPs (with average diameter of about 14 nm) at 520 nm [19]. After addition of $[RuCl(dppb)(bipy)(4\text{-}vpy)]^+$ (4×10^{-4} mol L^{-1} in acetone) to the colloidal suspension of AuNPs (0.05 mol L^{-1}), it was observed an enlarged band, centralized at 629 nm, with significant decrease of the original plasmon band of $AuNPs^-$ at 520 mn. The polarization of the conduction electron oscillations in adjacent AuNPs causes a red-shift on the plasmon absorbance, attributed to the coupling of plasmon absorbance of the particles [46,47]. Additional amounts of $[RuCl(dppb)(bipy)(4\text{-}vpy)]^+$ decrease the plasmon band even more, until the metal-ligand charge transfer (MLCT) of the ruthenium complex arises at 410 nm.

Aggregates of gold nanoparticles with ruthenium complexes can be obtained as a powder (Ru–AuNPs) after addition of excess of the cationic ruthenium complex into colloidal suspension of AuNPs. A formation of a quantitative precipitate occurs, and it can be collected by centrifugation and dried under vacuum.

The morphological and compositional analysis by electron microscopy was realized with $[RuCl(dppb)(bipy)(py)]^+$ and $AuNPs^-$, which produces a brown precipitate labeled as Rupy–AuNPs, as a result of the electrostatic interactions. The Rupy–AuNPs were investigated by SEM and TEM microscopy, both coupled to EDS detectors, as present in the Figs. 4 and 5.

SEM images of the resulting precipitate Rupy–AuNPs (Fig. 4A) reveals that precipitate is an assembly of AuNPs and the ruthenium complex, observed as round-shaped bright spots. These results are accordingly to our previous observations published [19]. The chemical composition of the precipitate was determined by the energy dispersed spectroscopy (EDS), as shown in Fig. 4B. The peaks of Ru, Cl, C, N, P and Au elements are observed (other peaks originated from the substrate). This suggests that the precipitated formed consists in a self-assembly of ruthenium cationic specimen and $AuNPs^-$.

Due the hydrophobic characteristic of the complexes containing ruthenium aggregates onto the surface of $AuNPs^-$, the Rupy–AuNPs are insoluble in water. Afterward the Rupy–AuNPs were dispersed in isopropanol and analyzed by TEM. The TEM images in the Fig. 5A shown that the Rupy–AuNPs were partially dissolved in isopropanol, leaving the AuNPs with average diameter about 20 nm (darker particles) and irregular shaped particles of ruthenium complex. With higher magnification (Fig. 5A below) it is possible to observe the coalescence of some AuNPs. This result suggests that the interactions between the cationic ruthenium complex and $AuNPs^-$ are non-covalent, and Rupy–AuNPs are acting as a salt. AuNPs do not change the structure and the electronic stability in solution of the applied ruthenium complex, because the $^{31}P\{^1H\}$ NMR and cyclic voltammetry data are the same in the

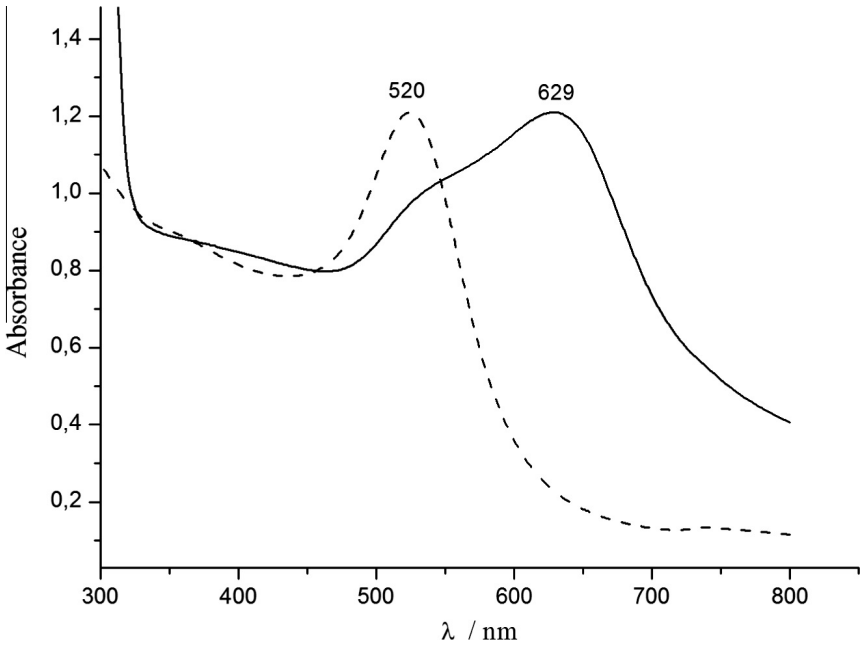

Fig. 3. Interaction of AuNPs and $[RuCl(dppb)(bipy)(4\text{-}vpy)]^+$ accompanied by UV–Vis. (dashed line) colloidal suspension of AuNPs (0.05 mol L^{-1}). (solid line) after addition of 600 μL of $[RuCl(dppb)(bipy)(4\text{-}vpy)]^+$ 4×10^{-4} mol L^{-1} in acetone.

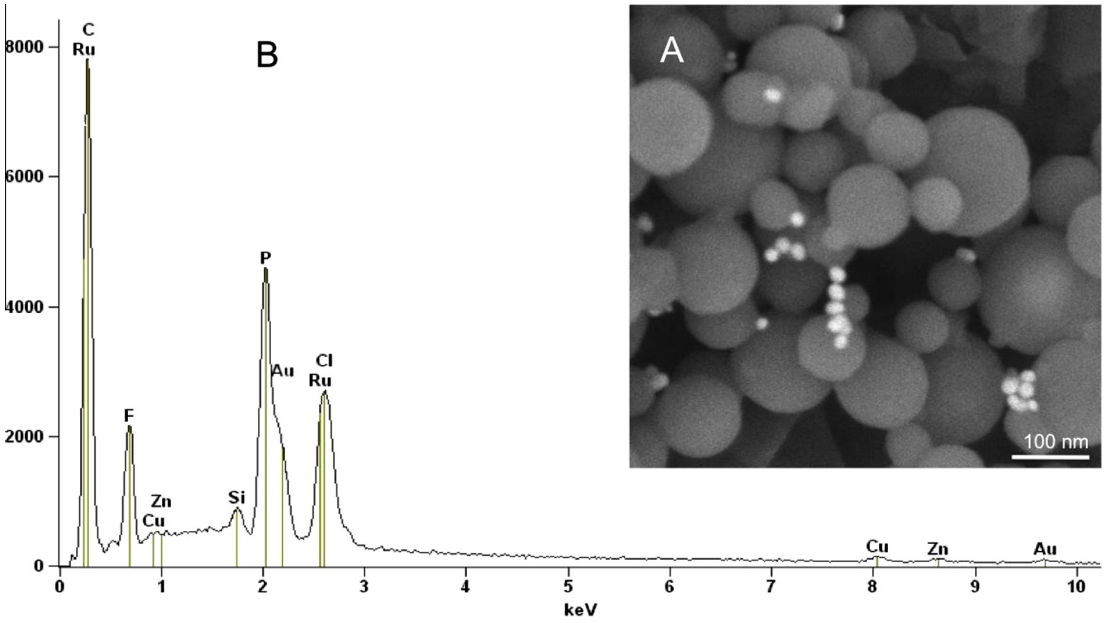

Fig. 4. (A) SEM image and (B) corresponding EDS spectrum of the resulting precipitate Rupy–AuNPs {Rupy = $[RuCl(dppb)(bipy)(py)]^+$}.

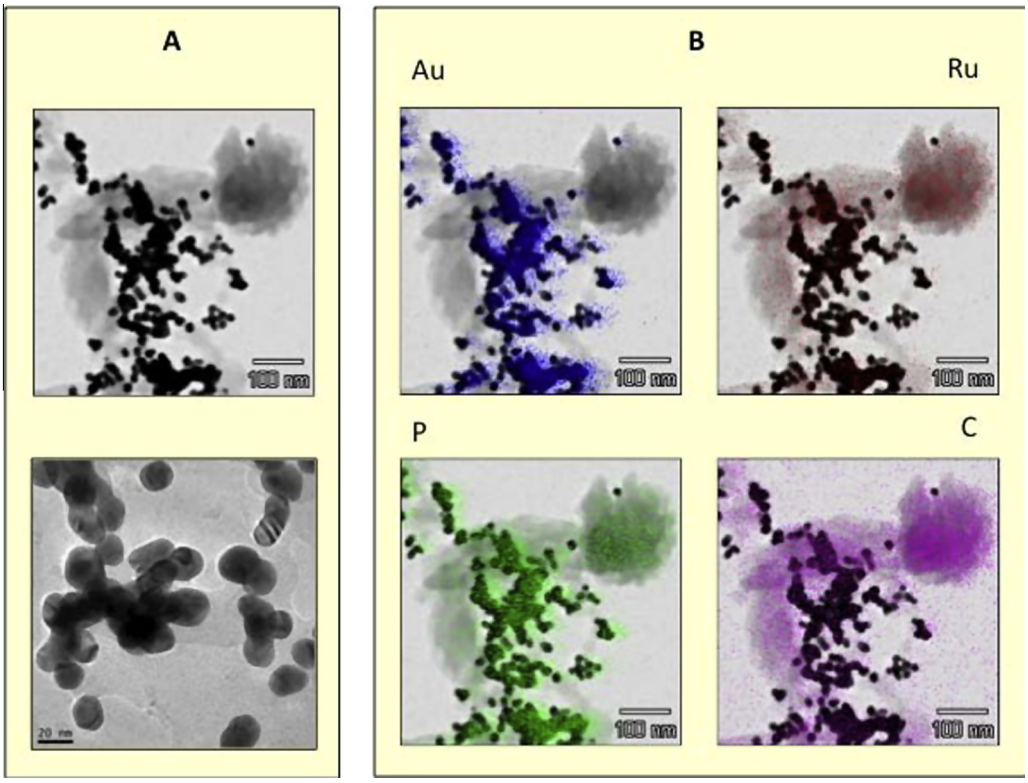

Fig. 5. (A) TEM images of Rupy–AuNPs dissolved in isopropanol {Rupy = $[RuCl(dppb)(bipy)(py)]^+$}. (B) TEM elemental maps related to Au, Ru, P and C elements.

presence and absence of AuNPs [19]. It is an important observation to use the Ru–AuNPs species as a new material for further application.

The Fig. 5B shows the elemental mappings obtained by EDS–STEM mode of Rupy–AuNPs dispersed in isopropanol, with the distribution of Au, Ru, P and C in the STEM image. The Au mapping confirms the AuNPs presence in the material as the spherical dark spots. The slight shift observed on the elemental mappings is due to a drift of the sample during scanning acquisition. Ru, P and C are related to the ruthenium coordination complex and C is also related to the citrated-capped AuNPs. The distribution mapping also confirms the partial dissolution process of the solid in isopropanol. It is important to notice the P mapping, such as Ru mapping, are very close to the AuNPs mapping, suggesting the permanence of the ruthenium complex in the anionic species, after partially dissolution in isopropanol.

3.2. Modified glassy carbon electrode with AuNPs using [RuCl(dppb)(bipy)(4-vpy)]$^+$ as crossed linking agent

A thin film of [RuCl(dppb)(bipy)(4-vpy)]$^+$ was generated onto the surface of glassy carbon electrode (GCE), using cyclic voltammetry, under potential cycling between −2.4 and +2.0 V, to produce the CGE–Ru$^+$. An adsorption wave process of the 4-vpy occurs at −1.2 V, and reduction waves processes at −1.6 and −2.1 V. Similar potential related to adsorption and reduction processes of vinyl group were observed by Franco and coworkers [48] in the electropolymerization of *trans*-[$RuCl_2$(4-vpy)$_4$] on Au, Pt and glassy carbon electrodes. Cyclic voltammetry of [$RuCl_2$(4-vpy)$_4$] shows the vinyl reduction waves at the −1.5 and −2.45 V range and adsorption wave around −0.8 V. Fig. 6 present the cyclic voltammogram of [RuCl(dppb)(bipy)(4-vpy)]$^+$, under potential cycling between 2.0 and −2.4 V, in dichloromethane solution of TBAH (0.1 mol L^{-1}), using a working GCE, a Pt counter electrode, and Ag/AgCl electrode as reference. Typical Ru (III/II), oxidation/reduction wave are also observed at 1.16 and 1.05 respectively ($E_{½}$ = 1.10 V), and vinyl reduction waves were observed in the cathodic processes.

After 10 voltammetry cycles the GCE–Ru$^+$ electrode was obtained and it was kept in a colloidal suspension of AuNPs for 1 h to incorporate them on the surface of GCE–Ru$^+$ by electrostatic interaction. The resulting electrode GCE–Ru–AuNPs was finally washed with water and used for the detection of acetaminophen by cyclic voltammetry.

3.3. Acetaminophen detection using CGE–Ru–AuNPs

The anodic peak current (I_{pa}) response using GCE–Ru–AuNPs electrode to acetaminophen detection increases with pH, reaching a maximum at pH 5.5, and then decreases at alkaline pH. The anodic peak potential (E_{pa}) response is also dependent of pH conditions, which indicates that the electrochemical reaction involves a proton transfer. In the case of acetaminophen oxidation to N-acetyl-*p*-quinoneimine, two electrons and two protons process are involving [49,50].

Cyclic voltammogram obtained in CH_3COONa solution (0.1 mol L^{-1}), without pH controlled, containing acetaminophen in different concentration (99–654 μmol L^{-1}) showed a linear relationship between the I_{pa} and the acetaminophen concentration, which can be described by the Eq. (1) and Fig. 7. The sensibility (S) and detection limit (DL) values were respectively:

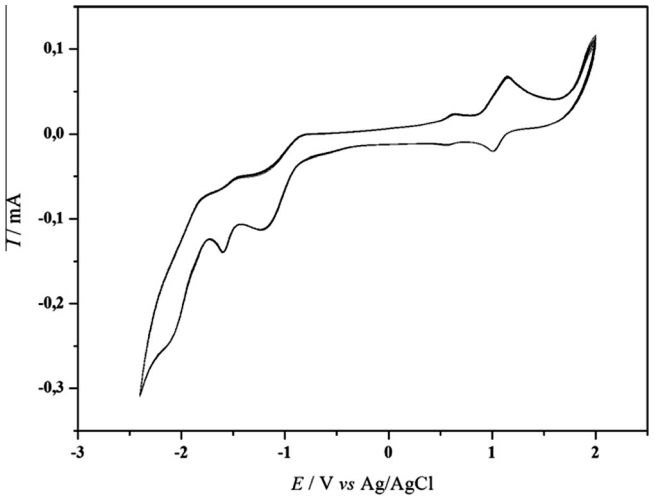

Fig. 6. Thin film of [RuCl(dppb)(bipy)(4-vpy)]$^+$ generated onto the surface of glassy carbon electrode, scan rate = 100 mV/s, 10 cycles under potential cycling between 2.0 and −2.4 V in dichloromethane solution of TBAH (0.1 mol L^{-1}).

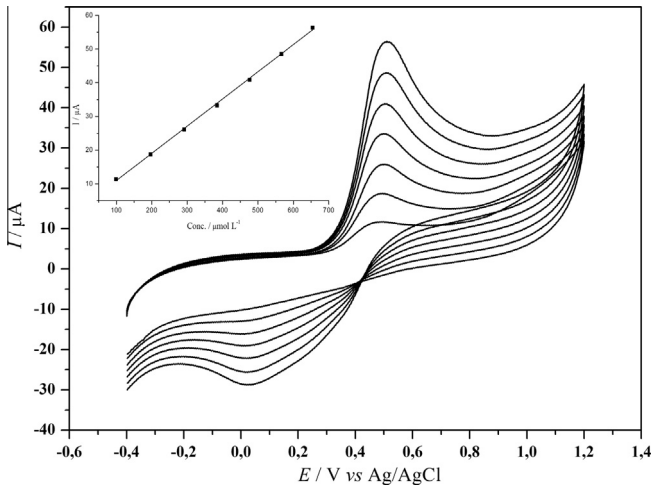

Fig. 7. A) Cyclic voltammograms obtained with GCE–Ru–AuNPs in CH_3COONa solution (0.1 mol L^{-1}) containing acetaminophen in different concentrations (99–654 μmol L^{-1}). Scan rate of 100 mV s^{-1}. B) Linear relationship between I_{pa} (μA) and acetaminophen concentration (μmol L^{-1}).

0.083 μA μmol L^{-1} and 1.08 μmol L^{-1}. DL values were obtained as follows: DL = 3sd/S, where sd = standard deviation of three blank measures.

$$I_{pa}(\mu A) = 2.062 + 0.083C(\mu molL^{-1})(C \text{ in } \mu molL^{-1}, R^2 = 0.999) \quad (1)$$

The cyclic voltammogram response, using 0.01 mol L^{-1} of acetaminophen in GCE–Ru–AuNPs, was measured using different scan rates over 50–550 mV s^{-1} range. The E_{pa} varied linearly with the square root of the scan rate, indicating that the electrochemical reaction is a diffusion-controlled process, as described by Eq. (2).

$$I_{pa}(\mu A) = -10.89 + 12.36(mVs^{-1})^{1/2}(v \text{ in } mVs^{-1}, R^2 = 0.999) \quad (2)$$

In Fig 8, using pH controlled at 5.5, it is possible to observe the electrochemical behavior of the GCE and GCE–Ru–AuNPs in the acetaminophen detection, and in the Table 2 the reversibility electrochemical parameters. The redox potential reversibility (ΔE_p) of acetaminophen with GCE–Ru–AuNPs was improved 3.6 times when compared to GCE, and the I_{pa} and I_{pc} were improved 1.43 and 1.67 times respectively. The stability of GCE–Ru–AuNPs was

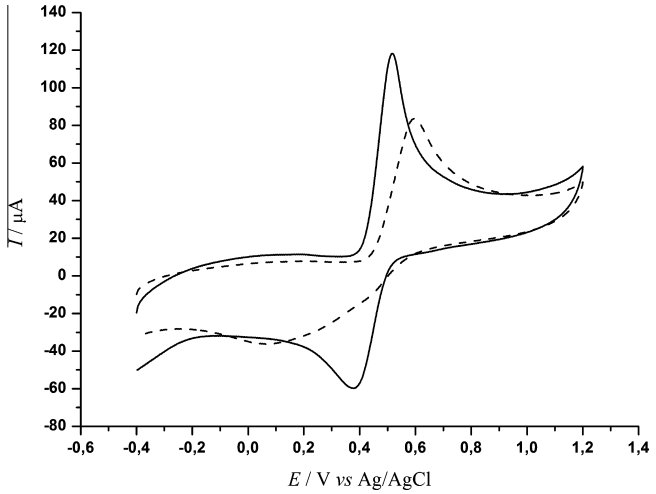

Fig. 8. Cyclic voltammograms using GCE (dashed line) and GCE–Ru–AuNPs (solid line) for acetaminophen detection (0.01 mol L^{-1}) in CH_3COONa (0.1 mol L^{-1}) solution as the electrolyte support at pH 5.5.

Table 2
Reversibility voltammograms parameters to acetaminophen detection: GCE and GCE–Ru–AuNPs.

Electrochemical parameters	GCE	GCE–Ru–AuNPs
E_{pa} (V)	0.548	0.515
E_{pc}(V)	0.084	0.386
ΔE_p (V)	0.464	0.129
I_{pa} (μA)	82.422	117.822
I_{pc} (μA)	−35.394	−59.242

tested for 5 successive measurements of 0.01 mol L^{-1} acetaminophen in CH_3COONa (0.1 mol L^{-1}) solution at pH 5.5. Relative standard deviations (RSDs) of E_{pa} and I_{pa} responses were 0.19% and 0.50% respectively, which suggests that the GCE–Ru–AuNPs has high stability.

4. Conclusions

The interaction between $[RuCl(dppb)(bipy)(py)]^+$ and $AuNPs^-$ was accompanied by SEM–EDS and TEM–EDS measurements, indicating to be electrostatic interactions. Therefore it was used to add AuNPs onto the surface of glassy carbon electrode (GCE), without Au–S covalent bond. In toward of this view, a thin film of $[RuCl(dppb)(bipy)(4\text{-}vpy)]^+$ was generated onto the surface of glassy carbon electrode (GCE), using cyclic voltammetry, by adsorption and reduction of 4-vinylpyridine group. This step produced a glassy carbon–Ru^+ electrode (GCE–Ru^+), which was used to incorporate a stable gold nanoparticles (AuNPs), with desired shapes and sizes on the surface of electrode, by electrostatic interaction between GCE–Ru^+ and $AuNPs^-$ (GCE–Ru–AuNPs). The performances of the GCE□ and GCE–Ru–AuNPs were evaluated by cyclic voltammetry for acetaminophen determination, having the latter a high stability (Relative standard deviations (RSDs) of E_{pa} and I_{pa} responses were 0.19% and 0.50% respectively). The redox potential reversibility (ΔE_p) of acetaminophen with GCE–Ru–AuNPs was improved by almost four times when compared to the GCE; also, the E_{pa} response increases with the increase of the acetaminophen concentration at pH 5.5.

Acknowledgement

We thank FAPEMIG, CNPq, CAPES, FAPESP, FINEP and RQ-MG for financial support.

Appendix A. Supplementary data

CCDC 987996 contains the supplementary crystallographic data for the complex $[RuCl(dppb)(5,5'\text{-Me-}2,2'\text{-bipy})(4\text{-vpy})]PF_6$. These data can be obtained free of charge via http://www.ccdc.cam.ac.uk/conts/retrieving.html, or from the Cambridge Crystallographic Data Centre, 12 Union Road, Cambridge CB2 1EZ, UK; fax: (+44) 1223 336 033; or e-mail: deposit@ccdc.cam.ac.uk.

References

[1] P. Zhao, N. Li, D. Astruc, Coord. Chem. Rev. 257 (2013) 638.
[2] Z. Wang, L. Ma, Coord. Chem. Rev. 253 (2009) 1607.
[3] G. Frens, Nat. Phys. Sci 241 (1973) 20.
[4] J. Turkevich, P.C. Stevenson, J. Hillier, Faraday Soc. 11 (1951) 55.
[5] M. Brust, M. Walker, D. Bethell, D.J. Schiffrin, R. Whyman, J. Chem. Soc., Chem. Commun. (1994) 801.
[6] M. Brust, F. Fink, D. Bethell, D.J. Schiffrin, C.J. Kielly, J. Chem. Soc., Chem. Commun. (1995) 1655.
[7] E. Rampazzo, S. Bonacchi, D. Genovese, R. Juris, M. Marcaccio, M. Montalti, F. Paolucci, M. Sgarzi, G. Valenti, N. Zaccheroni, L. Prodi, Coord. Chem. Rev. 256 (2012) 1664.
[8] N. Yan, C. Xiao, Y. Kou, Coord. Chem. Rev. 254 (2010) 1179.
[9] M.-C. Daniel, D. Astruc, Chem. Rev. 104 (2004) 293.
[10] C.M. Niemeyer, Angew. Chem., Int. Ed. 40 (2001) 4128.
[11] E. Katz, I. Willner, Angew. Chem., Int. Ed. 43 (2004) 6042.
[12] N.L. Rosi, C.A. Mirkin, Chem. Rev. 105 (2005) 1547.
[13] M.E. Stewart, C.R. Anderton, L.B. Thompson, J. Maria, S.K. Gray, J.A. Rogers, R.G. Nuzzo, Chem. Rev. 108 (2008) 494.
[14] J.W. Steed, D.R. Turner, K.J. Wallace, Core Concepts in Supramolecular Chemistry and Nanochemistry, John Wiley & Sons Ltd, England, 2007.
[15] X. Sun, Y. Du, S. Dong, E. Wang, Anal. Chem. 77 (2005) 8166.
[16] H. Wei, J. Yin, E. Wang, Anal. Chem. 80 (2008) 5635.
[17] A.N. Shipway, M. Lahav, R. Gabai, I. Willner, Langmuir 16 (2000) 8789.
[18] M. Lahav, A.N. Shipway, I. Willner, J. Chem. Soc., Perkin Trans. 2 (1999) 1925.
[19] K.M. de Oliveira, T.C.C. dos Santos, L.R. Dinelli, J.Z. Marinho, R.C. Lima, A.L. Bogado, Polyhedron 50 (2013) 410.
[20] M.C.R. Monteiro, F.B. Nascimento, E.M.A. Valle, J. Ellena, E.E. Castellano, A.A. Batista, S.P. Machado, J. Braz. Chem. Soc. 21 (10) (1992) 2010.
[21] M.I.F. Barbosa, E.M.A. Valle, S.L. Queiroz, J. Ellena, E.E. Castellano, V.R.S. Malta, J.R. Sousa, O. Piro, M.P. Araujo, A.A. Batista, Polyhedron 29 (2010) 2297.
[22] A.A. Batista, S.L. Queiroz, G. Oliva, M.T.P. Gambardella, R.H.A. Santos, B.R. James, Inorg. Chim. Acta 267 (1998) 209.
[23] A.A. Batista, K. Wohnrath, E.E. Castellano, I.S. Moreira, J. Elena, L.R. Dinelli, M.P. Araujo, J. Chem. Soc., Dalton Trans. 19 (2000) 3383.
[24] A.A. Batista, M.O. Santiago, C.L. Donnici, I.S. Moreira, P.C. Healy, S.B. Price, S.L. Queiroz, Polyhedron 20 (2001) 2123.
[25] Enraf-Nonius COLLECT, Nonius BV, Delft: The Netherlands, 1997–2000.
[26] Z. Otwinowski, W. Minor, W. Macromol. Crystallogr., PT A, 276 (1997) 307.
[27] R.H. Blessing, Acta Crystallogr. Sect. A 51 (1995) 33.
[28] G.M. Sheldrick, SHELXS-97. Program for Crystal Structure Resolution. University of Göttingen, Göttingen, Germany, 1997.
[29] G.M. Sheldrick, SHELXL-97. Program for Crystal Structures Analysis. University of Göttingen, Göttingen, Germany, 1997.
[30] L.J. Farrugia, J. Appl. Crystallogr. 30 (1997) 565.
[31] E.R. dos Santos, M.A. Mondeli, L.V. Pozzi, R.S. Corrêa, H.S. Salistre-de-Araújo, F.R. Pavan, C.Q.F. Leite, J. Ellena, V.R.S. Malta, S.P. Machado, A.A. Batista, Polyhedron 51 (2013) 292.
[32] M.I.F. Barbosa, E.R.D. Santos, A.E. Graminha, A.L. Bogado, L.R. Texeira, H. Beraldo, M.T.S. Trevisan, J. Ellena, E.E. Castellano, B.L. Rodrigues, M.P. de Araujo, A.A. Batista, Polyhedron 30 (2011) 41.
[33] J. Wolf, S. Wolfram, W.H. Grünwald, P. Scwab, M. Schulz, Angew. Chem. 37 (1998) 1124.
[34] A.L. Bogado, R.M. Carlos, C. Daólio, A.G. Ferreira, M.G. Neumann, F. Rominger, S.P. Machado, J.P. da Silva, M.P. de Araujo, A.A. Batista, J. Organomet. Chem. 696 (2012) 4184.
[35] L.L. Romualdo, A.L. Bogado, E.M.A. Valle, I.S. Moreira, J. Ellena, E.E. Castellano, M.P. de Araujo, A.A. Batista, Polyhedron 27 (2008) 53.
[36] E.M.A. Valle, B.A.V. Lima, A.G. Ferreira, F.B. Do Nascimento, V.M. Deflon, I.C.N. Diógenes, U. Abram, J. Ellena, E.E. Castellano, A.A. Batista, Polyhedron 28 (2009) 3478.
[37] T.F. Gallati, A.L. Bogado, G. Von Poelhsitz, J. Ellena, E.E. Castellano, A.A. Batista, M.P. De Araujo, J. Organomet. Chem. 692 (2007) 5447.
[38] D.A. Cavarzan, F.D. Fagundes, O. Fuganti, C.W.P. da Silva, C.B. Pinheiro, D.F. Back, A. Barison, A.L. Bogado, M.P. de Araujo, Polyhedron 62 (2013) 75.
[39] E.M.A. Valle, F.B. Nascimento, A.G. Ferreira, A.A. Batista, M.C.R. Monteiro, S.P. Machado, J. Ellena, E.E. Castellano, E.R. Azevedo, Quim. Nova 31 (2008) 807.
[40] M.P. de Araujo, A.T. de Figueiredo, A.L. Bogado, G. Von Poelhsitz, J. Ellena, E.E. Castellano, C.L. Donnici, J.V. Comasseto, A.A. Batista, Organometallics 24 (2005) 6159.
[41] G.N. Coleman, J.W. Gesler, F.A. Shirley, J.R. Kuempel, Inorg. Chem. 12 (1973) 1036.
[42] G. Von Poelhsitz, A.L. Bogado, L.M., A.G. Ferreira, E.E. Castellano, J. Ellena, A.A. Batista, Polyhedron 29 (2010) 280.
[43] L.R. Dinelli, G. Von Poelhsitz, E.E. Castellano, J. Ellena, S. Galembeck, A.A. Batista, Inorg. Chem. 48 (2009) 4692.
[44] R.N. Sampaio, W.R. Gomes, D.M.S. Araujo, A.E.H. Machado, R.A. Silva, A. Marletta, I.E. Borissevitch, A.S. Ito, L.R. Dinelli, A.A. Batista, S.C. Zílio, P.J. Gonçalves, N.M. Barbosa, Neto, J. Phys. Chem. 116 (2012) 18.
[45] S.L. Queiroz, A.A. Batista, G. Oliva, M.T. Gambardella, R.H. Santos, K.S. Macfarlane, S.J. Rettig, B.R. James, Inorg. Chim. Acta 267 (1998) 209.
[46] Y. Yang, S. Matsubara, M. Nagomi, J. Shi, Mater. Sci. Eng., B 140 (2007) 172.
[47] H.E. Toma, V.M. Zamarion, S.H. Toma, K. Araki, J. Braz. Chem. Soc. 21 (2010) 1158.
[48] M.C.E. Bandeira, J.A. Crayston, N.S. Gonçalves, L.K. Noda, A. Glidle, C.V. Franco, J. Solid State Electrochem. 11 (2007) 231.
[49] Z. Xu, Q. Yue, Z. Zhuang, D. Xiao, Microchim. Acta 164 (2009) 387.
[50] M.M. da Silva, G.H. Ribeiro, A.A. Batista, A.M. de Faria, A.L. Bogado, L.R. Dinelli, J. Braz. Chem. Soc. 24 (2013) 1772.